A genetic locus required for iron acquisition in *Mycobacterium tuberculosis*

R. Krithika*, Uttara Marathe*, Priti Saxena, Mohd. Zeeshan Ansari, Debasisa Mohanty, and Rajesh S. Gokhale†

Chemical Biology Group, National Institute of Immunology, Aruna Asaf Ali Marg, New Delhi 110 067, India

Edited by Christian R. H. Raetz, Duke University, Durham, NC, and accepted by the Editorial Board December 16, 2005 (received for review September 10, 2005)

Mycobactins are a family of membrane-associated siderophores required for *Mycobacterium tuberculosis* to adapt to its intracellular habitat. These lipophilic siderophores have been recently shown to directly acquire intracellular iron through lipid trafficking. Despite tremendous progress in understanding the assembly-line enzymology of the siderophore biosynthesis, the genes as well as the mechanistic and biochemical principles involved in producing membrane-associated siderophores have not been investigated. Here, we report a biosynthetic locus that incorporates variety of aliphatic chains on the mycobactin skeleton. Cell-free reconstitution studies demonstrate that these acyl chains are directly transferred from a carrier protein on to the ε-amino group of lysine residue by an unidentified Rv1347c gene product. The unsaturation in the lipidic chain is produced by a novel acyl-acyl carrier protein dehydrogenase, which, in contrast to the conventional acyl-CoA dehydrogenases, is involved in the biosynthetic pathway. MbtG protein then performs the final N6-hydroxylation step. Genome-wide analysis revealed homologues of *N*-acyl transferase and MbtG in other pathogenic bacteria. Because iron plays a key role in the development of infectious diseases, the biosynthetic pathway described here represents an attractive target for developing new antibacterial agents.

biosynthesis | mycobactin | siderophore | acyl-transferase | dehydrogenase

Many bacterial pathogens, due to limited availability of free iron in the host, secrete siderophores to establish and maintain infection. Because iron is an essential cofactor for several enzymatic processes, restricting the availability of iron is an important strategy for defense against bacterial infections (1, 2). Siderophores are typically low molecular weight peptidic metabolites that are specifically induced in response to low iron concentrations (3, 4). To date, several hundred siderophores have been isolated and characterized that vary considerably in chemical composition. In recent years a novel family of cell-associated amphiphilic siderophores has been recognized in marine bacteria (5, 6) (Fig. 1). Interestingly, such membrane-associated siderophores that contain a lipidic side chain attached to a polar head group were first characterized from mycobacteria several years ago (7). The availability of microbial genome sequences has propelled our understanding of the assembly-line enzymology of siderophore biosynthesis (8). However, the molecular components of the biosynthetic machinery involved in the assembly of lipophilic siderophores remain to be elucidated.

Mycobacterium tuberculosis, which survives within the phagosomes of macrophages, competes for host iron by producing both soluble and lipophilic iron acquisition systems (9, 10). Mycobactins have been considered to be intra-envelope short-term storage molecules that interact with soluble carboxymycobactins for accessing host iron pools (11). In a recent study, the lipophilic mycobactins were shown to directly acquire intracellular iron through lipid trafficking (12). It has been proposed that the ferric mycobactins preferentially localize at lipid droplets, which are then delivered to phagosomes. The *apo*-form of mycobactin supposedly folds into a more compact spherical head group upon iron binding, which results in the decreased membrane affinity of the siderophore. Previous studies of the interactions of the amphiphilic siderophore marinobactin E and its iron complexes with phospholipid vesicles have suggested that the membrane affinity of siderophores could also be modulated by the unsaturation in the fatty acid tail and the carbon chain length (13). Together, these studies have emphasized the critical function of lipidic moiety in modulating the membrane permeability and dynamic diffusibility of lipophilic siderophores that are crucial for iron sequestration.

Genetic disruption studies along with *in vitro* characterization of MbtA and the N-terminal domain of MbtB have confirmed that *mbt* cluster from *M. tuberculosis* is involved in production of siderophores (14, 15). Based on sequence homologies of the *mbt*-encoded proteins and the modular logic of nonribosomal peptide synthetases, a biosynthetic scheme for mycobactin formation has been proposed (9, 10). However, genes encoding the enzymes responsible for transferring the acyl substitutions of different aliphatic chain lengths and for introducing unusual cis double bond conjugated to carbonyl group that distinguish mycobactin and carboxymycobactin are not found in the *mbt* cluster and have not been identified in the mycobacterial genome. In this study, we have identified a genetic locus involved in the assembly of mycobactins, which we propose to annotate as *mbt-2*. Interestingly, several genes from the *mbt-2* cluster were earlier demonstrated to be essential for the growth of mycobacteria (16, 17). Our studies here delineate the biochemical functions of all these genes. Cell-free reconstitution studies provide molecular mechanistic insights of how acyl chains are directly transferred from a carrier protein on to the ε-amino group of lysine residue by an unidentified Rv1347c gene product. The unsaturation in the lipidic chain is produced by an acyl-acyl carrier protein (ACP) dehydrogenase (FadE14), which, in contrast to the conventional acyl-CoA dehydrogenases, is involved in this biosynthetic pathway. We also demonstrate that MbtG protein performs the N6-hydroxylation step to generate functionally important hydroxamate moieties. Furthermore, our genome-wide analysis reveals homologues of *N*-acyl transferase (NAT) as well as N6-monooxygenase from several pathogenic bacteria. This report of the biochemical reconstitution reveals unique molecular components of siderophore biosynthetic machinery that are crucial for iron sequestration during bacterial pathogenesis.

Results

Computational Analysis of Iron-Dependent Genes Regulated by IdeR Repressor. The transcriptional profiling studies of iron-dependent genes in *M. tuberculosis* have revealed several genes

BIOCHEMISTRY

Conflict of interest statement: No conflicts declared.

This paper was submitted directly (Track II) to the PNAS office. C.R.H.R. is a guest editor invited by the Editorial Board.

Abbreviations: ACP, acyl carrier protein; ESI, electrospray ionization; PMS, phenazine methosulfonate.

*R.K. and U.M. contributed equally to this work.

†To whom correspondence should be addressed. E-mail: rsg@nii.res.in.

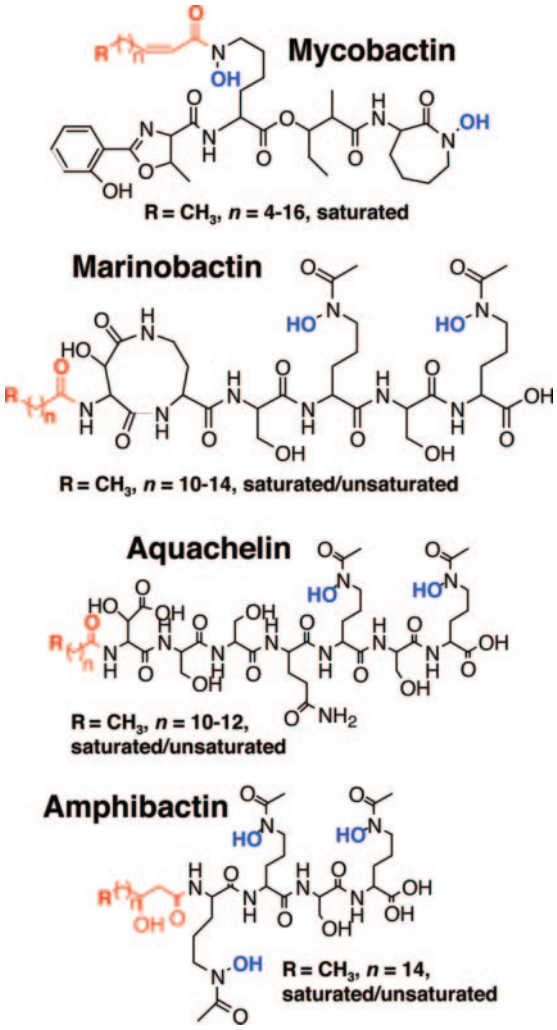

Fig. 1. Structures of amphiphilic siderophores: Mycobactin from *M. tuberculosis*, marinobactin from *Marinobacter sp.*, aquachelin from *H. aquamarina*, and amphibactin from *Vibrio* sp. R-10.

required for iron acquisition and storage that are regulated by IdeR repressor (18). Because *mbt* biosynthetic cluster is regulated by IdeR repressor, we carefully analyzed other genes that could impart amphiphilicity to mycobactins and whose expression is modulated by the levels of iron in the growth medium. One such interesting cluster contains proteins (FadD33 and FadE14) that showed distinct homology to proteins involved in lipid metabolism. The disruption of *fadD33* gene in *M. tuberculosis* H37Rv had earlier suggested the important role of the gene product in mycobacterial virulence by supporting its replication in the liver (17). Computational analysis of FadD33 protein indicated that this protein was homologous to the newly discovered fatty acyl-AMP ligase (FAAL) proteins from mycobacteria (19). Our recent biochemical studies showed that these closely related FadD proteins convert fatty acids into their corresponding acyl adenylates, which are transferred on to the phosphopantetheine arm of carrier proteins. Interestingly, Rv1344, the ORF neighboring *fadD33*, shows similarity to acyl carrier protein. FadE14 is homologous to acyl-CoA dehydrogenases that typically catalyze the dehydrogenation of acyl-CoA thioesters to the corresponding *trans*-2-enoyl-CoA (20, 21). The position of active site *Glu* residue in the protein sequence is analogous to typical medium-/long-chain acyl-CoA dehydrogenases. The adjacent Rv1347c gene in the mycobacterial genome is transcribed in the opposite direction and shows homology to aerobactin siderophore biosynthesis protein IucB (22). The recent determination of complete genome sequence of *Nocardia farcinica* IFM 10152 also revealed a protein with high sequence similarity to Rv1347c (23). Remarkably, this gene in *Nocardia* is present besides other putative siderophore genes. Threading results of Rv1347c gene product using Genthreader suggested that this hypothetical protein has homology to histone acetyltransferases (HATs) (24), which transfer the acetyl group on to the ε-amino group of lysine residue. We therefore predicted that this protein indeed may be involved in the acylation of lysine residues in mycobactin. In a very recent report, the 3D structure of Rv1347c gene product was determined as part of the mycobacterial structural genomics initiative; however, its biological function has not yet been established (25).

Organization of these four genes across several mycobacterial species clearly showed complete conservation in *Mycobacterium microti*, *Mycobacterium avium*, *Mycobacterium smegmatis*, *Mycobacterium bovis*, *Mycobacterium marinum*, and *Mycobacterium ulcerans*, but not in *Mycobacterium leprae*. Recently, the transposon-mediated mutagenesis in *M. smegmatis* had indicated an essential role of Rv1345 gene product in mycobactin biosynthesis (26). Intriguingly, complementation with corresponding genes from *M. tuberculosis* failed to restore mycobactin synthesis in *M. smegmatis*, despite its high degree of sequence homology. To test our predictions, we decided to directly probe the biochemical functions of all these proteins by cell-free reconstitution studies.

Biochemical Investigations of the New *mbt* Cluster: FadD33 Activates Lipidic Moieties Required for Mycobactin Biosynthesis. Expression of FadD33 protein in *Escherichia coli* primarily resulted in the formation of inclusion bodies. Addition of lauroyl sarcosine (10 mM) during cell lysis provided 20–30% protein in soluble fraction (Fig. 2*A*). The enzymatic activity of FadD33 was tested by using a variety of medium-/long-chain fatty acids. The formation of acyl adenylate was confirmed by combination of HPLC and MS analysis, as described (27). Because there is a putative ACP (Rv1344) domain present in this cluster, we explored whether this carrier protein could be charged with aliphatic fatty acids. *In vitro* acylations with radiolabeled substrates confirmed that the ACP protein could be posttranslationally modified by promiscuous surfactin phosphopantetheinyl transferases (sfp) (28). The inclusion of *holo*-ACP in the FadD33 reaction assays resulted in the formation of lauroylated-ACP (Fig. 2*B*). Nanospray MS analysis showed a molecular ion peak $[M + H]^+$ at m/z 14002.82 consistent with molecular formula of *His*-tagged lauroyl-ACP protein.

Rv1347c Directly Transfers Long Chain Acyl Moieties from the Carrier Protein onto the Mycobactin Core. The next step in the assembly of amphiphilic mycobactin would involve N-acylation of these ACP tethered long-chain fatty acids directly onto the ε-amino group of lysine. We investigated whether Rv1347c protein could perform this final catalytic step using substrate mimics. The benzyloxycarbonyl lysine methyl ester (Z-Lys-OMe; I) was chemically synthesized and was used as surrogate substrate for the deacylated form of mycobactin (Fig. 2*B*). The α-amino group of lysine is acylated by benzyloxy carbonyl group and possesses only a free ε-amino group. Analysis of the reaction products formed during the incubation of Z-Lys-OMe along with ^{14}C-lauroyl-CoA and Rv1347c protein by using radio-TLC showed formation of two new products with an approximate R_f of 0.5 and 0.4 (k_{obs} 24.5 min^{-1}) (Fig. 2*C*). These metabolites were analyzed on HPLC and characterized as *N*6-lauroyl Z-Lys-OMe (II) and *N*6-lauroyl Z-Lys-OH by electrospray ionization tandem MS (ESI-MS/MS). The identity of product was also confirmed by the synthesis of chemical reference. Further investigations with the ACP-tethered intermediates, instead of acyl-CoAs, showed good

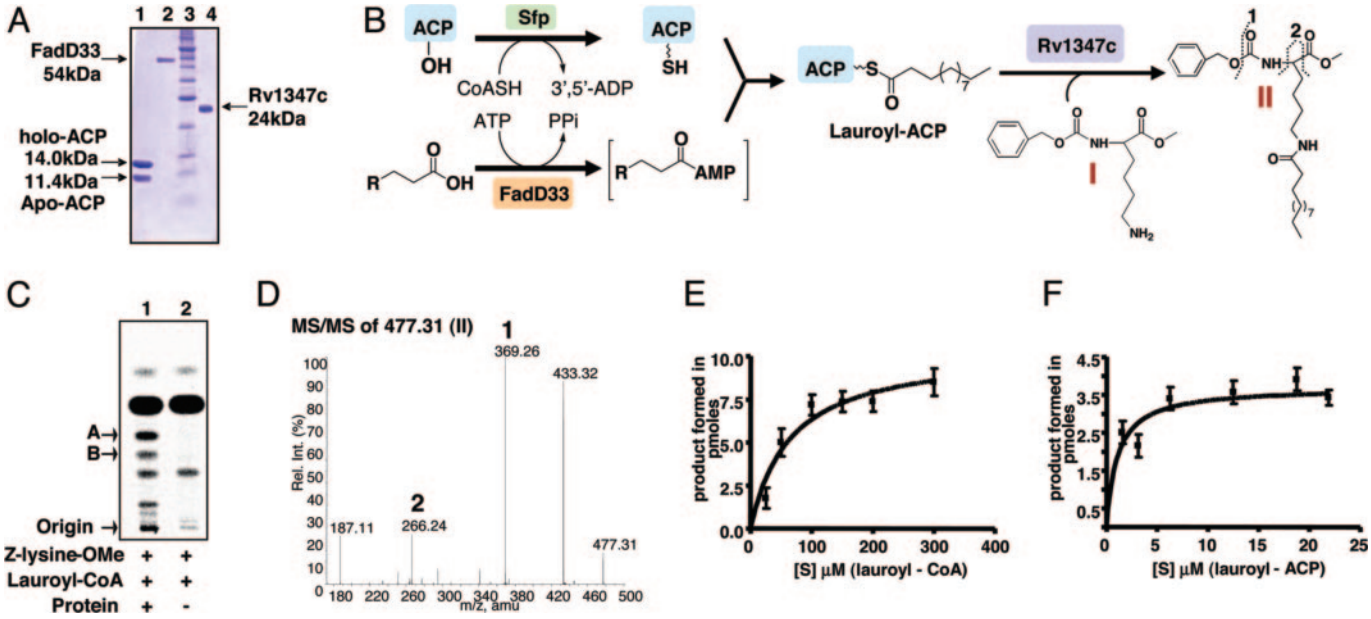

Fig. 2. Activation and transfer of acyl chains onto the ε-amino group of lysine. (*A*) SDS/PAGE profiles of purified Rv1344 (ACP), FadD33, and Rv1347c proteins. Two ACP bands were observed corresponding to the *apo*- and *holo*-forms of protein. (*B*) FadD33-mediated activation of fatty acid and transfer onto the phosphopantetheinylated ACP. The lauroyl moiety bound to the ACP domain is transferred to the ε-amino group of the Z-lysine-OMe (I) by Rv1347c protein. (*C*) Radio-TLC analysis of Rv1347c-catalyzed enzymatic activity yielded two radioactive bands corresponding to *N*6-lauroyl Z-lysine methyl ester (band A) and *N*6-lauroyl Z-lysine (band B). These products were not observed in the absence of the protein. (*D*) MS/MS analysis of *N*6-lauroyl Z-lysine-OMe (II). The fragmentation sites are marked in dots on the chemical structure. (*E* and *F*) Steady-state kinetic measurements of Rv1347c protein for lauroyl-CoA and lauroyl-ACP.

catalytic rates for the formation of *N*6-lauroyl Z-Lys-OMe, and MS analysis showed molecular ion peak $[M + H]^{+1}$ at 477.31 (Fig. 2*D*). The comparison of steady-state kinetic parameters for the formation of lauroyl-Lys products by using lauroyl-CoA and lauroyl-ACP substrates suggested an apparent K_M of 34 μM and 0.72 μM, respectively (Fig. 2 *E* and *F*). This ≈50-fold difference between the affinities for these two substrates clearly demonstrates that Rv1347c protein prefers ACP-bound substrates over CoA-esters. Examination of substrate specificity showed that this protein could transfer a wide range of medium- to long-chain fatty acids (C_6–C_{16}). Kinetic analysis with Rv1347c clearly showed higher specificity for long-chain fatty acyl-CoAs, as compared with their K_M values (Table 1).

FadE14 Is an Acyl-ACP Dehydrogenase. Because Rv1347c showed affinity for ACP-bound intermediates, we wanted to investigate whether acyl-CoA dehydrogenase homologue FadE14 would also use similar substrates. The catalytic cycle of acyl-CoA dehydrogenase results in the simultaneous reduction of cofactor FAD to $FADH_2$. To regenerate the oxidized form of the cofactor, the two widely used electron acceptors phenazine methosulfonate (PMS) and ferricenium hexafluorophosphate ($Fc^+PF^-_6$) were independently used as in the enzymatic assays (29). The ACP-tethered substrates showed no activity with PMS, whereas catalytic turnover was observed with $Fc^+PF^-_6$ (k_{obs} 120 min^{-1}). The inability of PMS to support the catalytic activity was not investigated further. Because $Fc^+PF^-_6$ provided robust activity, this was used in this study. The α,β-unsaturated aliphatic chains bound to ACP were subsequently transferred on to ε-amino group of Z-Lys-OMe by using Rv1347c protein (Fig. 3*A*). The final product was extracted and analyzed by ESI-MS/MS. The TOF-MS spectra clearly showed a molecular ion peak $[M + H]^+$ at m/z 475.35 (Fig. 3*B*), which is 2 Da less than the *N*6-lauroyl Z-Lys-OMe (II). Furthermore, the collision-based fragmentation of 475.35 yielded fragments of 367.24 and 181.15, which could be observed only for dehydrogenated *N*6-lauroyl Z-Lys-OMe. These studies clearly demonstrate that FadE14 can introduce a double bond on the ACP-tethered products.

Table 1. Steady-state kinetic analysis for Rv1347c protein

Acyl-CoA	K_M, μM
Hexanoyl-CoA	166.20
Decanoyl-CoA	86.12
Lauroyl-CoA	33.93
Palmitoyl-CoA	19.50

Results are means (n = 3) with SE values <15%.

MbtG Produces Hydroxamate Groups in Mycobactin Necessary for Iron Sequestration. Although the precise order in which terminal steps would occur in mycobactin biosynthesis is not clear, the recent isolation of didehydroxymycobactins (DDMs) from the early-infected cultures of *M. tuberculosis* had suggested that lysine hydroxylation may be the final step in the mycobactin assembly (30). The *mbtG* gene product from the *mbt* cluster has been anticipated to be a lysine *N*6-hydroxylase (9, 15). Previous studies with *N*6-hydroxylase from aerobactin biosynthetic cluster had suggested that these proteins belong to the family of flavoprotein monooxygenases and consume molecular oxygen during catalysis (31, 32). The enzymatic reactions with MbtG protein were carried out with *N*6-lauroyl Z-Lys-OMe (II) in the presence of NADPH and FAD, in air saturated buffers (Fig. 4*A*). Under these conditions, MbtG protein showed low catalytic turnover (k_{obs} 3.2 min^{-1}). The MS analysis of the extracted products showed a molecular ion peak $[M + H]^+$ at m/z 493.48. The ESI-MS/MS yielded fragments, which clearly indicated the hydroxylated product of the acylated lysine (Fig. 4*B*). Hydroxylation activity of MbtG protein was also detected with L-lysine. The competition experiment showed 5-fold preference for using acetylated lysine over lysine. MbtG protein also displayed spec-

BIOCHEMISTRY

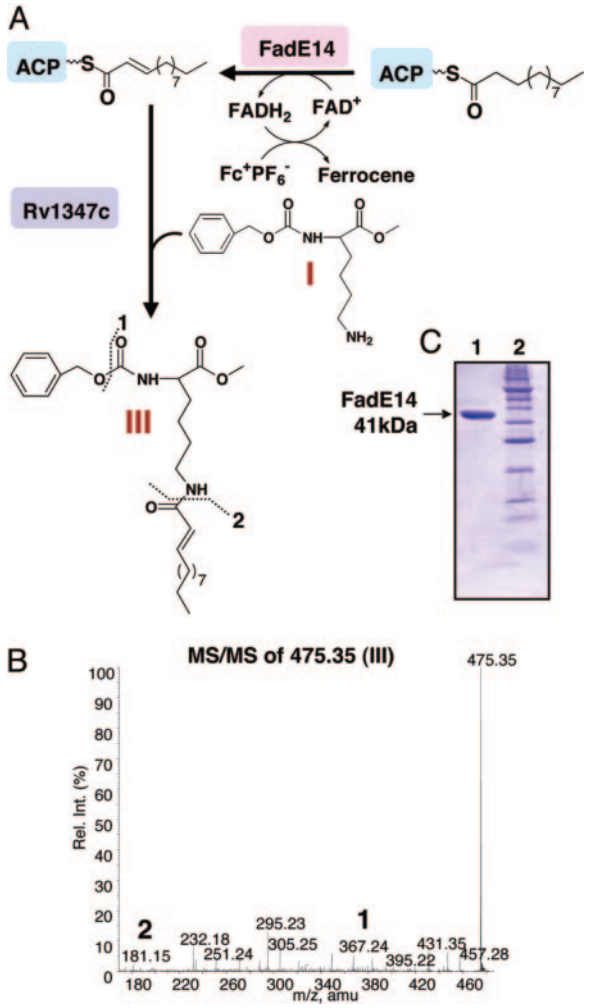

Fig. 3. Enzymatic activity of FadE14 protein. (*A*) FadE14 catalyzes the dehydrogenation at the α-β position of ACP-bound acyl chains, which can be further transferred to Z-lysine-OMe (I) by Rv1347c protein to produce (III). (*B*) Tandem MS analysis of the dehydrogenated product (III). (*C*) FadE14 could be purified to homogeneity as a 41-kDa protein.

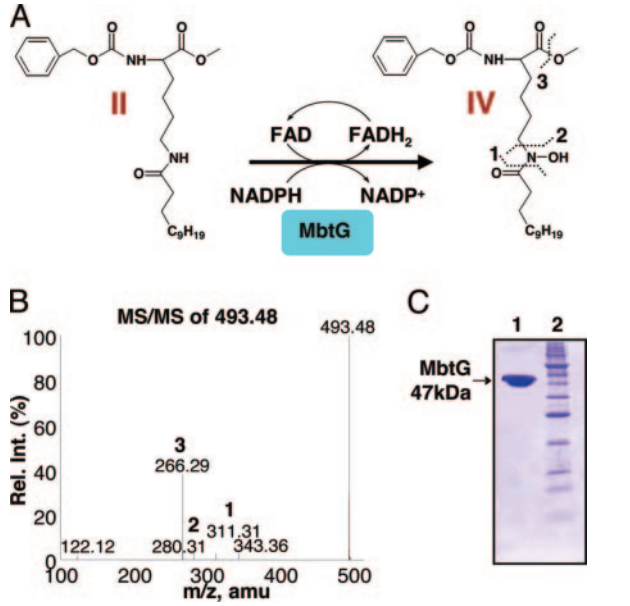

Fig. 4. Hydroxylation of ε-amino group of lysine. (*A*) MbtG is a flavoprotein monooxygenase that utilizes FAD and NADPH as cofactors to perform hydroxylation reactions. (*B*) Positive ion MS analysis of the product (IV) generated a molecular ion at 493.48. The MS/MS produced *m*/*z* peak at 311.31, which is obtained by the loss of the lauroyl moiety. Some of the other fragment ions generated during collisional fragmentation are also shown here. (*C*) SDS/PAGE of purified MbtG protein.

ificity for the side chain amino group and no hydroxylation was observed at α-amino group.

Discussion

Our cell-free reconstitution studies provide evidence for the direct involvement of this peripheral cluster in the biosynthesis of mycobactin. We propose to annotate this cluster as *mbt-2*, whereas the earlier identified cluster involved in the synthesis of mycobactin core may be referred to as *mbt-1*. Both these clusters are transcriptionally regulated by iron concentrations using IdeR repressor. We show that the *mbt-2* cluster dictates the incorporation of lipophilic aliphatic chain to produce amphiphilic metabolites (Fig. 5). Based on the existing nomenclature, the four genes from this cluster can be annotated as *mbtK*, *mbtL*, *mbtM*, and *mbtN* for *Rv1347c*, *Rv1344*, *fadD33*, and *fadE14*, respectively. It is interesting to note that even the tailoring steps in the mycobactin biosynthesis proceed on acyl-*S*-enzyme intermediates. The preferred utilization of acyl-*S*-enzyme intermediates by MbtK and MbtN may be an efficient method to channelize substrates and thereby provide an effective mechanism to generate specificity during the biosynthesis of metabolites.

It is worthwhile to note that both *mbtK* and m*btG* genes were found to be essential for the growth of *M. tuberculosis* in a genome-wide mutational analysis (33). Homologues of these two genes could also be identified from various other pathogenic organisms, including *Burkholderia cepacia*, *Pseudomonas*, *Nocardia*, *Acetinobacter*, and *Sinorhizobium meliloti*. Structural analysis of *N*-acyl transferase proteins from different organisms suggested variations in the acyl chain-binding pocket. Interestingly, *Nocardia farcinica* produces siderophore nocobactin that differs from mycobactin primarily in terms of acetyl modification at the lysine residue. Our molecular modeling studies suggest two crucial aliphatic residues (*Pro*145 and *Ala*183) in the substrate-binding pocket of MbtK that are replaced to relatively hydrophilic side chains in *Nocardia N*-acyl transferase protein. It is possible that these two residues may be important in determining the specificity of acyl chain length. However, MbtK protein showed exclusive specificity to acylate at the ε-amino position, and the amino group at α-position was not readily modified. Interestingly, this protein was able to acylate the δ-position of ornithine amino acid and also catalyzed transfer of acyl chains on to gramicidin S, which contains two ornithine residues.

In an earlier study, an acyl-CoA dehydrogenase homologue (FkbI) from FK520 PKS cluster was speculated to use ACP-bound substrates, based on its 3D structure (34). However, no confirmation for such a catalytic activity was established. In this study, we have characterized an acyl-ACP dehydrogenase activity for MbtN protein that is involved in the biosynthesis of a metabolite. This result is in contrast to widely distributed CoA-using acyl-CoA dehydrogenases that are primarily involved in β-oxidation degradative pathway (20, 21). Because acyl-CoA dehydrogenases, in general, are known to catalyze formation of trans-isomer and mycobactins contains a cis double bond, it would be worthwhile to investigate the stereochemistry of FadE14 reaction. It would be interesting to study whether protein–protein interactions between ACP and FadE14 might facilitate the formation of an unusual geometry at the α-β position. Bioinformatics analysis of the mycobacterial genome

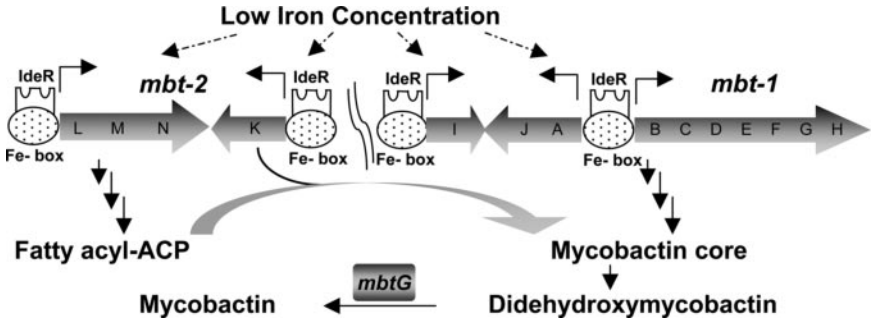

Fig. 5. Biosynthetic scheme of the proposed pathway for amphiphilic mycobactins. During low iron conditions, the IdeR-Fe^{2+} complex is not formed, which results in the activation of transcription of IdeR-repressed genes (38). The iron box promoters (Fe-box) are found adjacent to both *mbt-1* and *mbt-2* clusters whereas *mbt-1* gene cluster produces mycobactin skeleton and *mbt-2* cluster produces acyl-*S*-ACP intermediates. These acyl-*S* intermediates are then transferred to produce didehydroxymycobactin in the presence of MbtK. The final hydroxylation is carried out by MbtG to generate the amphiphilic mycobactin siderophore.

did not reveal any apparent cis-trans isomerase in the proximity of these two *mbt* clusters.

MbtG belongs to flavoprotein monooxygenases that generate hydroxamate unit, a common iron-binding functional group present in siderophores. Homologues of MbtG proteins are present in a number of siderophore-producing organisms. Disruption of these monooxygenases in *Burkholderia cepacia*, *Aspergillus nidulans* and *Aspergillus fumigatus* results in loss of effective persistence and colonization and has been proposed to be absolutely essential for virulence (35, 36). In *B. cepacia*, the siderophore biosynthesis was partially restored by addition of *N*-hydroxy ornithine to the cultures (37). Interestingly, the didehydroxy analog of mycobactin siderophore has been recently isolated from mycobacteria, suggesting that hydroxylation may be the last step in biosynthesis (30). It is interesting to note that the mechanism of N-hydroxylations along with nonribosomal biosynthesis of siderophore backbone has been conserved throughout the bacterial evolution and may indicate the role of lateral gene transfer in the siderophore biosynthetic pathway. Because iron plays a key role in the development of infectious diseases, the biosynthetic enzymes described in this study represent outstanding candidates as targets for developing antibacterial agents against tuberculosis and related bacterial diseases.

Materials and Methods

A bacterial artificial chromosome library of *M. tuberculosis H37Rv* was obtained from the Pasteur Research Institute (Paris). Radioactive materials were purchased from Amersham Pharmacia Biosciences, PerkinElmer, and American Radiolabeled Chemicals (St. Louis). All other chemicals used were of analytical grade and were purchased from Sigma, New England Biolabs, Stratagene, and Merck.

Cloning, Expression, and Purification. Primers used for cloning various genes are as follows: *fadE14* (5′-*CATATG*ACGGCCGGCTCCGACCTC-3′ and 5′-*GAATTC*GCTTTGGAAGCTCCGAC-3′); *fadD33* (5′-*CATATG*AGTGAGCTCGCGGCCGTG-3′ and 5′-*GAATTC*TCAGTCCGCCATCTCCAGGGA 3′); *ACP* (5′-*CATATG*TGGCGATATCCACTAAGT-3′ and 5′-*GAATTC*TCAGAGCGGTATTTGGC-3′); *Rv1347c* (5′-*CATATG*ACCAAACCCACATCCGCT-3′ and 5′-*GAATTC*GCAGCCGTGGTCGGAGC-3′; and *mbtG* (5′-*CATATG*-AATCCGACGCTCGCGGTC-3′ and 5′-*GAATTC*TCAGCTAAAGGATTGGTGCTC-3′). These primers with engineered NdeI and EcoRI sites (italicized) were used to amplify the relevant genes by using a bacterial artificial chromosome genomic library. The *fadE14*, *ACP*, and *Rv1347c* were cloned in NdeI-EcoRI sites on pET21c for expression with C-terminal hexa-His-tag. The *mbtG* and *fadD33* were cloned in pET28c for expression as N-terminal hexa-His tag. All proteins were expressed by using BL21-DE3 strain of *E. coli*. Proteins were obtained in the soluble fraction by inducing cultures at low temperatures and IPTG concentrations. Expression of FadD33 protein in *E. coli* primarily resulted in the formation of inclusion bodies. Addition of lauroyl sarcosine (10 mM) during cell lysis provided 20–30% proteins in soluble fraction. These proteins were purified by Ni^{2+}-NTA affinity chromatography followed by anion exchange chromatography by using the AKTA (Amersham Pharmacia) chromatographic system. All proteins were purified to >97% homogeneity.

Enzyme Assays for FadD33. The enzymatic activity of FadD protein was analyzed by radio-TLC and HPLC, as described (18). Formation of acyl adenylate was confirmed by using ESI-MS.

Acylation of ACP. Acylation of mycobacterial Rv1344 *holo*-ACP was carried out by using FadD33/FadD28 protein, both of which make acyl adenylates (18). The reaction mixture contained 50 mM Tris (pH 6.8), 10 mM $MgCl_2$, 1 mM Tris-(2-carboxyethyl)phosphine (TCEP), 100 μM [^{14}C]lauroyl-CoA, and 5–10 μm ACP. Reaction mixture was incubated for 20 min at 30°C, and the lauorylated-ACP was purified by using Ni^{2+}-NTA affinity chromatography. This lauroylated-ACP along with Z-lysine-OMe were used as substrates for Rv1347c protein.

Characterization of Rv1347c. The acylated product of Rv1347c protein was analyzed by radio-TLC. The reaction mixture included 50 mM Tris (pH 8.0), 100 μM [^{14}C]acyl CoA, 1 mM Z-lysine-OMe, and 20 μM protein in a 50-μl reaction volume. The reaction was initiated by the addition of Rv1347c protein and incubated for 30 min at 30°C. The products were extracted with ethyl acetate, concentrated, and analyzed by TLC by using a solvent system of 4:1 ethyl acetate/hexane. The radiolabeled product was detected by using PhosphorImager (Fuji BAS5001). A control reaction without protein was carried out to monitor the rate of spontaneous acylation of Z-lysine-OMe from acyl-CoA. Extracted product was analyzed by ESI-MS.

Kinetic Analysis of Rv1347c. Reactions were carried out as described above with varying concentrations (15–400 μM) of [^{14}C]acyl-CoAs. Reactions were initiated with the addition of protein and incubated for 3 min at 30°C. Products were extracted and resolved on TLC as described above. Fuji BAS5001 PhosphorImager was used to quantitate the radiolabeled products.

Chemical Synthesis of Standard. *N*-α-benzyloxycarbonyl-L-lysine methyl ester hydrochloride was synthesized by using standard Fmoc (9-fluorenylmethoxycarbonyl) chemistry (38) and was

later on purchased from Novabiochem. *N*6-lauroyl Z-lysine-OMe was synthesized by using Schotten-Baumann conditions (39). Z-lysine-OMe (200 mg, 0.68 mmol) was dissolved in 20 ml of pyridine, and lauroyl chloride (297 mg, 1.36 mmol) was added to this solution. The reaction was carried out for 6 h at room temperature. The product was then extracted with ethyl acetate and washed with water. The product was first detected by using TLC and then purified on a C5 reverse phase Phenomenax HPLC column. Formation of the product was confirmed by MS analysis, $(M + H)^+$ 477.3328 (C23H16O4N calculated 476.3250).

Enzyme Assay for FadE14. Dehydrogenase activity was carried out by using PMS and ferricenium hexafluorophosphate as electron acceptors. The reaction volume consisted of 50 mM Tris (pH 7.6), 0.5 mM lauroyl-ACP, 250 μM ferricenium hexafluorophosphate (or 3 mM PMS), 100 μM FAD, and 30 μg of protein. The reaction was started by the addition of FadE14, and the contents were incubated for 30 min at 30°C. The dehydrogenated product was then transferred onto the ε-amino group of Z-lysine-OMe mediated by Rv1347c. Products were extracted by using ethyl acetate and analyzed by MS.

Enzymatic Activity of MbtG. Reactions were carried out with 100 μM Z-lauroyl lysine-OMe, 100 mM Tris (pH 7.0), 100 μM FAD, 150 μM NADPH, and 20 μg of MbtG. Contents were incubated at 30°C for 1 h, extracted with ethyl acetate, and confirmed by MS. In the competition experiments, lysine concentration was varied from 75 μM to 500 μM.

We thank Pooja Arora for technical help and analysis and Dr. Sandip K. Basu for helpful discussions. M.Z.A. is a Senior Research Fellow of the Council of Scientific and Industrial Research, India. R.S.G. is a Wellcome Trust International Senior Research Fellow in India and also a Howard Hughes Medical Institute International Fellow. This work was also supported by grants to the National Institute of Immunology by the Department of Biotechnology (DBT), India.

1. Ferreras, J. A., Ryu, J. S., Di Lello, F., Tan, D. S. & Quadri, L. E. N. (2005) *Nat. Chem. Biol.* **1,** 29–32.
2. Fluckinger, M., Haas, H., Merschak, P., Glasgow, B. J. & Redl, B. (2004) *Antimicrob. Agents Chemother.* **48,** 3367–3372.
3. Andrews, S. C., Robinson, A. K. & Rodriguez-Quinones, F. (2003) *FEMS Microbiol. Rev.* **27,** 215–237.
4. Schaible, U. E. & Kaufmann, S. H. (2004) *Nat. Rev. Microbiol.* **2,** 946–953.
5. Martinez, J. S., Carter-Franklin, J. N., Mann, E. L., Martin, J. D., Haygood, M. G. & Butler, A. (2003) *Proc. Natl. Acad. Sci. USA* **100,** 3754–3759.
6. Martinez, J. S., Zhang, G. P., Holt, P. D., Jung, H. T., Carrano, C. J., Haygood, M. G. & Butler, A. (2000) *Science* **287,** 1245–1247.
7. Snow, G. A. (1970) *Bacteriol. Rev.* **34,** 99–125.
8. Crosa, J. H. & Walsh, C. T. (2002) *Microbiol. Mol. Biol. Rev.* **66,** 223–249.
9. De Voss, J. J., Rutter, K., Schroeder, B. G. & Barry, C. E., 3rd (1999) *J. Bacteriol.* **181,** 4443–4451.
10. Ratledge, C. (2004) *Tuberculosis (Edinburgh)* **84,** 110–130.
11. Gobin, J. & Horwitz, M. A. (1996) *J. Exp. Med.* **183,** 1527–1532.
12. Luo, M., Fadeev, E. A. & Groves, J. T. (2005) *Nat. Chem. Biol.* **1,** 149–153.
13. Xu, G., Martinez, J. S., Groves, J. T. & Butler, A. (2002) *J. Am. Chem. Soc.* **124,** 13408–13415.
14. De Voss, J. J., Rutter, K., Schroeder, B. G., Su, H., Zhu, Y. & Barry, C. E., 3rd. (2000) *Proc. Natl. Acad. Sci. USA* **97,** 1252–1257.
15. Quadri, L. E., Sello, J., Keating, T. A., Weinreb, P. H. & Walsh, C. T. (1998) *Chem. Biol.* **5,** 631–645.
16. Sassetti, C. M., Boyd, D. H. & Rubin, E. J. (2003) *Mol. Microbiol.* **48,** 77–84.
17. Rindi, L., Fattorini, L., Bonanni, D., Iona, E., Freer, G., Tan, D., Deho, G., Orefici, G. & Garzelli, C. (2002) *Microbiology* **148,** 3873–3880.
18. Rodriguez, G. M. & Smith, I. (2003) *Mol. Microbiol.* **47,** 1485–1494.
19. Trivedi, O. A., Arora, P., Sridharan, V., Tickoo, R., Mohanty, D. & Gokhale, R. S. (2004) *Nature* **428,** 441–445.
20. Ghisla, S. & Thorpe, C. (2004) *Eur. J. Biochem.* **271,** 494–508.
21. Kim, J. J. & Miura, R. (2004) *Eur. J. Biochem.* **271,** 483–493.
22. de Lorenzo, V., Bindereif, A., Paw, B. H. & Neilands, J. B. (1986) *J. Bacteriol.* **165,** 570–578.
23. Ishikawa, J., Yamashita, A., Mikami, Y., Hoshino, Y., Kurita, H., Hotta, K., Shiba, T. & Hattori, M. (2004) *Proc. Natl. Acad. Sci. USA* **101,** 14925–14930.
24. McGuffin, L. J., Bryson, K. & Jones, D. T. (2000) *Bioinformatics* **16,** 404–405.
25. Card, G. L., Peterson, N. A., Smith, C. A., Rupp, B., Schick, B. M. & Baker, E. N. (2005) *J. Biol. Chem.* **280,** 13978–13986.
26. LaMarca, B. B., Zhu, W., Arceneaux, J. E., Byers, B. R. & Lundrigan, M. D. (2004) *J. Bacteriol.* **186,** 374–382.
27. Trivedi, O. A., Arora, P., Vats, A., Ansari, M. Z., Tickoo, R., Sridharan, V., Mohanty, D. & Gokhale, R. S. (2005) *Mol. Cell* **17,** 631–643.
28. Gokhale, R. S., Tsuji, S. Y., Cane, D. E. & Khosla, C. (1999) *Science* **284,** 482–485.
29. Lehman, T. C., Hale, D. E., Bhala, A. & Thorpe, C. (1990) *Anal. Biochem.* **186,** 280–284.
30. Moody, D. B., Young, D. C., Cheng, T. Y., Rosat, J. P., Roura-Mir, C., O'Connor, P. B., Zajonc, D. M., Walz, A., Miller, M. J., Levery, S. B., *et al.* (2004) *Science* **303,** 527–531.
31. Stehr, M., Smau, L., Singh, M., Seth, O., Macheroux, P., Ghisla, S. & Diekmann, H. (1999) *Biol. Chem.* **380,** 47–54.
32. Thariath, A., Socha, D., Valvano, M. A. & Viswanatha, T. (1993) *J. Bacteriol.* **175,** 589–596.
33. Sassetti, C. M., Boyd, D. H. & Rubin, E. J. (2001) *Proc. Natl. Acad. Sci. USA* **98,** 12712–12717.
34. Watanabe, K., Khosla, C., Stroud, R. M. & Tsai, S. C. (2003) *J. Mol. Biol.* **334,** 435–444.
35. Visser, M. B., Majumdar, S., Hani, E. & Sokol, P. A. (2004) *Infect. Immun.* **72,** 2850–2857.
36. Schrettl, M., Bignell, E., Kragl, C., Joechl, C., Rogers, T., Arst, H. N., Jr., Haynes, K. & Haas, H. (2004) *J. Exp. Med.* **200,** 1213–1219.
37. Sokol, P. A., Darling, P., Woods, D. E., Mahenthiralingam, E. & Kooi, C. (1999) *Infect. Immun.* **67,** 4443–4455.
38. Atherton E. & Sheppard, R. C. (1989) *Solid Phase Peptide Synthesis: A Practical Approach* (IRL, Oxford).
39. Jass, P. A., Rosso, V. W., Racha, S., Soundararajan, N., Venit, J. J., Rusowicz, A., Swaminathan, S., Livshitz, J. & Delaney, E. J. (2003) *Tetrahedron* **59,** 9019–9029.